ELSEVIER

Contents lists available at ScienceDirect

Radiation Physics and Chemistry

journal homepage: www.elsevier.com/locate/radphyschem



Fricke-gel dosimeter: overview of Xylenol Orange chemical behavior



G.M. Liosi^{a,*}, D. Dondi^b, D.A. Vander Griend^c, S. Lazzaroni^{b,d}, G. D'Agostino^d, M. Mariani^a

- ^a Department of Energy, Nuclear Engineering Division, Politecnico di Milano, Milano, Italy
- ^b Department of Chemistry, University of Pavia, via Taramelli 12, 27100 Pavia, Italy
- ^c Calvin College, Department of Chemistry and Biochemistry, Grand Rapids, MI, United States
- d Istituto Nazionale di Ricerca Metrologica (INRIM), Unit of Radiochemistry and Spectroscopy, c/o Department of Chemistry, University of Pavia, via Taramelli 12, 27100 Pavia, Italy

ARTICLE INFO

Keywords: Fricke dosimeter Radiation dosimetry Optical spectrometry Xylenol Orange

ABSTRACT

The complexation between Xylenol Orange (XO) and Fe^{3+} ions plays a key role in Fricke-gel dosimeters for the determination of the absorbed dose via UV–vis analysis. In this study, the effect of XO and the acidity of the solution on the complexation mechanism was investigated. Moreover, starting from the results of complexation titration and Equilibrium Restricted Factor Analysis, four XO- Fe^{3+} complexes were identified to contribute to the absorption spectra. Based on the acquired knowledge, a new $[Fe^{3+}]$ vs dose calibration method is proposed. The preliminary results show a significant improvement of the sensitivity and dose threshold with respect to the commonly used Abs vs dose calibration method.

1. Introduction

The Fricke-gel chemical dosimeter was developed to provide a suitable tool for pre-treatment 3D dosimetry in clinical radiotherapy. This dosimeter consists in an air-saturated acidic aqueous Fe²⁺ ions solution, dispersed into a tissue equivalent gel matrix. The radiation-induced oxidation of Fe²⁺ ions allows to correlate the dose to the Fe³⁺ ions concentration (Schreiner, 2004; Lepage and Jordan, 2010). Thanks to the addition of the Xylenol Orange (XO), a Fe³⁺complexing agent, the dosimetric signal can be measured by means of optical absorbance in the visible range. In fact, the XO ligand chelates the Fe³⁺ ions leading to the formation of strongly colored complexes that mainly absorb around 585 nm (Appleby and Leghrouz, 1991). Therefore, the dose response is defined as the ratio between the difference (before and after irradiation) in absorbance at 585 nm and the absorbed dose. Both disodium and tetrasodium XO salts proved to be suitable for dosimetric purposes.

Despite this dosimetrical system has already been tested for real clinical applications - using clinical beams of linear accelerators, using different dose rates etc. - (Gum et al., 2002; Schreiner, 2004; Doran, 2009; Lepage and Jordan, 2010; Baldock et al., 2010; Olding et al., 2010; Marrale et al., 2014; Cavinato et al., 2014; Alexander et al., 2015), several issues still need to be faced in order to achieve a suitable tool to be employed in the medical routine for pre-treatment verification. The chemical composition, the calibration method and the measurement procedure should be standardized and optimized in order to have a better accuracy, stability and reproducibility of the

dose evaluation. In particular, the XO chemical behavior and optical properties are affected by the diluent and the pH, as well as the purity of the XO ligand (Gay et al., 1999). In addition, the XO-Fe³⁺ absorption spectrum could be composed by many chemical species, resulting in inaccurate measurement of the absorbed dose, especially at low doses. In particular, the impurities, inevitably present due to the procedure of the synthesis, could compete with the XO for the Fe³⁺ ions complexation affecting the absorption spectra. Both optical artifacts and dose threshold effects in the Abs vs Dose calibration curve were observed as a function of the wavelength used for the analysis (Babic et al., 2008). Moreover, a dose response variability as a function of the total absorbed dose was highlighted (Liosi et al., 2015). These results suggest the presence of at least two complexes of XO-Fe³⁺ with different stoichiometric ratio (Lepage and Jordan, 2010). A better comprehension of the speciation mechanisms could lead to a more precise and accurate evaluation of the absorbed dose, especially at low doses (below 5 Gy).

For this purpose, in this work a systematic analysis was conducted on Fricke solutions in order to shine a light on the XO chemical properties and on the complexation with Fe³⁺ ions. Both disodium and tetrasodium XO salts were studied. In particular, the purity of the XO was investigated by means of HPLC and mass spectrometry. Moreover, since a XO molecule contains four acidic groups, the influence of the pH on the XO chemical behavior was studied.

Thanks to the acquired knowledge concerning the speciation mechanisms, a $[{\rm Fe}^{3+}]$ vs Dose calibration curve in the range 0–40 Gy has been obtained from the absorption spectra of irradiated Fricke

^{*} Corresponding author.

dosimeters. Therefore, the sensitivity and the precision of the dose evaluation were improved, and the dose threshold effects were limited.

2. Materials and methods

The chemicals employed for the experimental activities are: Ammonium Iron(III) Sulfate Dodecahydrate (F3629 - Sigma Aldrich), Ferrous Ammonium Sulfate (FAS) (F3754 - Sigma Aldrich), Sulfuric Acid (Carlo Erba Reagent grade 96% pure), Tetrasodium XO Salt (33825 - Sigma Aldrich) and Disodium XO Salt (52097 - Sigma Aldrich). All the solutions were prepared with ultrapure milliQ water.

In order to evaluate the purity of both disodium and tetrasodium XO salts, HPLC and direct-injection mass spectrometry analysis have been carried out. The work conditions adopted for the HPLC (Waters 1525 binary pump, 2487 dual λ absorbance detector) were: C18 column, 65% CH $_3$ CN, 35% H $_2$ O, 1 mL/min. The absorbance was measured at 435 nm. Both disodium and tetrasodium XO salts were dissolved in 25 mM H $_2$ SO $_4$. The direct-injection mass spectrometry was conducted with a Thermo Scientific system with optimized work condition: DEP: 0 mA \times 30 s, 1000 mA at 20 mA/sec for 90 s; EI ionization mode 70 eV; Ion source: 250 °C; mass range: 50–650 Da; Scan rate: 800.5 amu/sec.

The effect of the acidity on both disodium and tetrasodium salts was studied by means of spectrophotometric analysis conducted at different sulfuric acid concentration in the range 0–100 mM. The spectra were acquired at room temperature (20 $\pm\,2$ °C) with constant the ligand concentration.

For this preliminary analysis, the speciation mechanism of XO and Fe³⁺ ions has been studied in a simplified aqueous system, excluding the gel matrix. The so called "following the ligand" (Lewis et al., 2012) adopted procedure foresees to keep constant the ligand concentration and increasing step by step the metal ion concentration. The solutions were poured into quartz cuvettes (with an optical path of 0.5 cm) and the absorption spectra were acquired by means of UV-vis spectroscopy (HP 8425A diode array spectrophotometer). Solutions containing 0.165 mM XO were prepared in 25 mM and 50 mM of H₂SO₄. A concentrated solution of Fe3+ ions was prepared starting from the previous one, in order to maintain constant the ligand concentration. A proper amount of the Fe3+ concentrated solution was gradually added so as to obtain solutions with constant ligand concentration and increasing Fe3+ ions concentration in the range 0-0.3 mM (step of 0.01 mM). The solution was then gently agitated and the optical analysis was performed after 5 min to allow the achievement of chemical equilibrium. The absorption spectra were acquired in the range 200-800 nm with respect to a water sample as a reference. The deconvolution of the spectra were performed with SIVVU™ program, a nonlinear least-squares regression program for performing equilibrium-restricted factor analysis (Vander Griend et al., 2008).

Aqueous dosimeters were irradiated in the range 0–40 Gy with 60 Co gamma source (dose rate 0.14~kGy/h). The chemical composition of the dosimeters were: 0.165~mM XO, 0.5~mM FAS, 25~mM sulfuric acid. The optical analysis was performed 40 min after irradiation. Both irradiation and analysis were executed at room temperature.

3. Results

3.1. Study of XO impurities

In order to study the impurities present in the XO disodium and tetrasodium salts, HPLC analysis with UV-vis detector was performed. In the Fig. 1, the absorbance obtained at 435 nm versus the elution time is reported for both disodium and tetrasodium salts dissolved in 25 mM sulfuric acid. The latter was added in order to exclude the presence of deprotonated XO. A series of secondary peaks is present in addition to the main peak related to the XO (retention time of about 3.4 min). A higher purity can be observed for the disodium salt

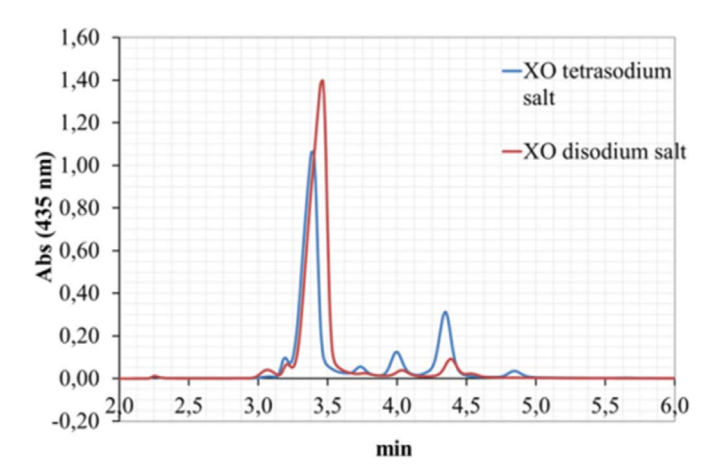


Fig. 1. Spectra obtained for both disodium and tetrasodium salts diluted in $25~\mathrm{mM}$ sulfuric acid. The absorbance at $435~\mathrm{nm}$ is reported as a function of the elution time.

probably due to a different synthesis procedure.

The mass spectra (Fig. 2) obtained by means of the direct-injection mass spectrometry allow to make assumptions on structural formula of different impurities having high molecular weight. The hypothesized structural formula makes reasonable to suppose their ability to compete with the XO for the complexation of the ferric ions with high absorption in the Vis range.

3.2. Effect of sulfuric acid concentration

Since XO molecule possesses four acidic groups, the possible complexing species could depend on pH. Several procedures for Fricke dosimeter preparation are reported in literature. The commonly adopted concentrations of sulfuric acid are 25 mM and 50 mM with both XO disodium and tetrasodium salt. For this reason, we decided to investigate the effect of different recipes on the XO acidic equilibrium.

The absorption spectra for both disodium and tetrasodium salts at 0, 25, 50 and 100 mM sulfuric acid were collected. The spectra obtained with the tetrasodium salt are reported in Fig. 3. Similar results are obtained for disodium salt. In the case of absence of sulfuric acid an absorption peak appears at 590 nm, probably due to the deprotonated XO. This peak disappears in the other acidic conditions showing that the ligand is completely protonated. It follows that XO anions are absent and the only complexing specie is the undissociated one.

3.3. Speciation mechanism

The speciation mechanism of XO and Fe^{3+} ions has been studied via complexation titration spectrophotometric analysis. In order to study the effect of the acidity both 25 mM and 50 mM sulfuric acid solution and XO disodium and tetrasodium were used. Since similar results were obtained, only the 25 mM sulfuric acid solution with the tetrasodium XO salt are discussed and reported hereafter. More than one isosbestic point is present (Fig. 4) so clearly the system is not comprised of just two components. For this reason, it is reasonable to suppose the presence of several XO-Fe $^{3+}$ complexes having different stoichiometric ratios.

In fact, the assumption of a 1:1 complex only gives a bad fitting of the data. For this reason was used the Equilibrium Restricted Factor Analysis approach (Vander Griend et al., 2008). This technique is a deconvolution of UV−Vis absorption spectra assuming that several XO-Fe³+ complexes can coexist and, with the fitting, the equilibrium constants can be evaluated. By means of SIVVU[™] program, it has been possible to properly deconvolute the absorption spectra in different components considering the real chemical equilibrium between species. Information concerning the stoichiometric ratio, equili-

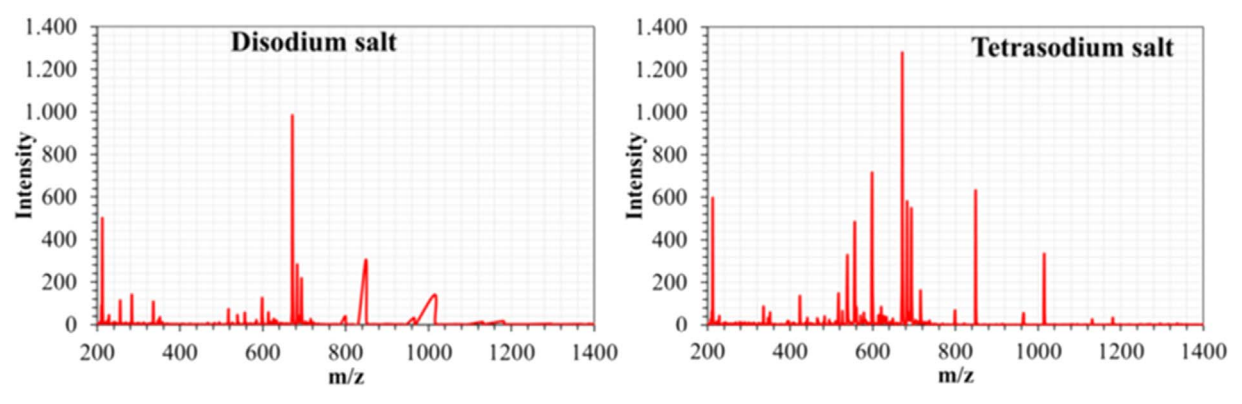


Fig. 2. Mass spectrums obtained for both disodium and tetrasodium salts.

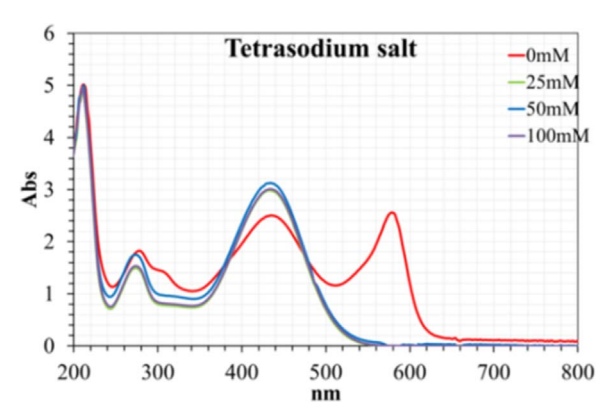


Fig. 3. Absorption spectra obtained at different acidic conditions for XO tetrasodium salt.

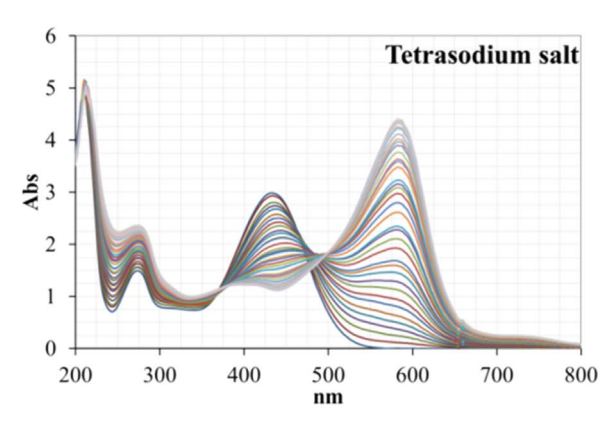


Fig. 4. Absorption spectra aquired at room temperature at increasing Fe^{3+} ions concentration and constant XO concentration.

brium constants and molar extinction coefficients were obtained (see Supplementary material). Four different complexes were identified for both disodium and tetrasodium salt: XO₃Fe, XO₂Fe, XOFe, XOFe₂. The complexes are in reciprocal equilibrium and their relative concentrations depend on the concentration of Fe³⁺ formed during the irradiation. The hypothesized chemical equilibriums are reported below:

$$3XO + Fe^{3+} \rightleftharpoons XO_3Fe$$

$$2XO_3Fe + Fe^{3+} \rightleftharpoons 3XO_2Fe$$

$$XO_2Fe + Fe^{3+} \rightleftharpoons 2XOFe$$

$$XOFe + Fe^{3+} \rightleftharpoons XOFe_2$$

	$\Delta G^{\circ} (kJ/mol)$	(log K)
XO ₃ Fe	-24.3(3)	4.3
XO_2Fe	-25.2(1)	4.46
XOFe	-78.7(8)	13.93
XOFe ₂	-68.0(8)	12.04

The calculated equilibrium constants of the complexes are reported in Table 1.

As it is visible from the values of logK, the most stable complex is the 1:1. Nevertheless, in order to have a good agreement with experimental data, also the other complexes should be considered.

3.4. Calibration method

Fricke dosimeters (25 mM sulfuric acid, and XO tetrasodium salt) were prepared and irradiated in the range 0–40 Gy. Subsequently two calibration curves Abs vs Dose at both 585 nm and 520 nm were obtained and plotted in Fig. 5. The curves show different sensitivities and dose thresholds as a function of the wavelength used for the fitting, as previously reported in literature (Babic et al., 2008).

As an alternative, we propose a calibration Conc vs. Dose based on the whole spectrum. To this aim, the concentration of the identified complexes are calculated by fitting the absorption spectrum starting from the computed molar extinction coefficients. The total concentration of Fe³⁺ ions is determined as a sum of the different components taking into account their stoichiometry. The obtained calibration curve, reported in Fig. 6, shows a significant reduction of the dose threshold and an enhancement of the sensitivity of about a factor of 2.

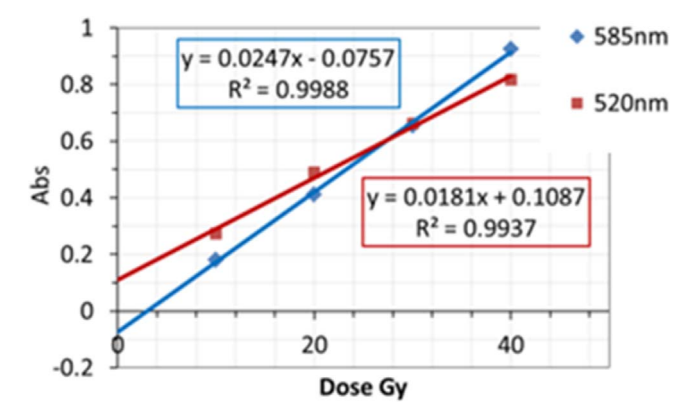


Fig. 5. Standard calibration Abs vs Dose obtained at 585 nm and 520 nm. Error bars are included in the marker size.

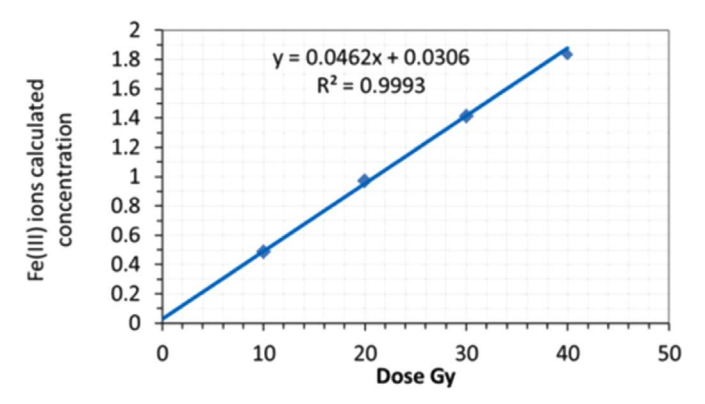


Fig. 6. Calibration curve which directly correlates $[Fe^{3+}]$ with the dose. Error bars are included in the marker size.

4. Conclusion

The XO impurities were analysed by means of HPLC and directinjection mass-spectrometry. High molecular weights impurities were detected for both disodium and tetrasodium XO even if with different concentrations. Nevertheless, this study did not show effects on the measured dose using the two salts.

Since the presence of XO anions was excluded, we focussed our speciation on undissociated XO molecules.

The study of the complexation identified four XO-Fe³⁺ complexes having different stoichiometry. In addition, the application of Equilibrium Restricted Factor Analysis approach allowed to determine their equilibrium constants and molar extinction coefficients. These data were used to obtain a [Fe³⁺] vs Dose calibration curve. A better sensitivity and a lower dose threshold were achieved with respect to the commonly adopted Abs vs Dose calibration curve.

The preliminary results obtained in this work are encouraging to apply the proposed methodology in the case of XO Fricke gel dosimeters.

Acknowledgments

This work has been supported by a co-funded Research Project (Politecnico di Milano and the Italian Ministry of education, University and Research MIUR) within the National Research Program of Relevant Interest (PRIN 2010) (Research Project no. 2010SNALEM_002). DVG acknowledges support by the National Science Foundation (grant number CHE-1310402), as well as the Camille & Henry Dreyfus Foundation (2014H Dreyfus Teacher-Scholar Award).

Appendix A. Supplementary material

Supplementary data associated with this article can be found in the online version at doi:10.1016/j.csr.2017.04.008.

References

Alexander, K.M., Pinter, C., Andrea, J., Fichtinger, G., Schreiner, L.J., 2015.
Implementation of an efficient workflow process for gel dosimetry using 3D Slicer.
Journal of Physics: Conference Series 573. In: Proceedings of the 8th International Conference on 3D Radiation Dosimetry (IC3DDose).

Appleby, A., Leghrouz, A., 1991. Imaging of radiation dose by visible color development in ferrous-agarose-Xylenol orange gels. Med. Phys. 18, 309–312.

Babic, S., Battista, J., Jordan, K., 2008. An apparent threshold dose response in ferrous xylenol-orange gel dosimeters when scanned with a yellow light source. Phys. Med. Biol. 53, 1637–1650.

Baldock, C., De Deene, Y., Doran, S., Ibbott, G., Jirasek, A., Lepage, M., McAuley, K.B., Oldham, M., Schreiner, L.J., 2010. Polymer gel dosimetry. Phys. Med. Biol. 55 (5),

Cavinato, C.C., Yoshizumi, M.T., Souza, B.H., Carrete Jr, H., Daros, R.B.M., Giordani, A. J., Rodrigues Jr, O., Campos, L.L., 2014. Comparative Study of the 3DCRT Dosimetric Response of Head Fricke Xylenol Gel Phantoms with and without Human Bone.

Doran, S.J., 2009. The history and principles of chemical dosimetry for 3-D radiation fields: gels, polymers and plastics. Appl. Radiat. Isot. 67 (3), 393–398.

Gay, C., Collins, J., Gebicki, J.M., 1999. Determination of iron in solutions with the ferric xylenol orange complex. Anal. Biochem. 273, 143–148.

Gum, F., Scherer, J., Bogner, L., Solleder, M., Rhein, B., Bock, M., 2002. Preliminary study on the use of an inhomogeneous anthropomorphic Fricke gel phantom and 3D magnetic resonance dosimetry for verification of IMRT treatment plans. Phys. Med. Biol. 47 (7), N67.

Lepage, M., Jordan, K., 2010. 3D dosimetry fundamentals: gels and plastics. J. Phys.: Conf. Ser., 250. http://dx.doi.org/10.1088/1742-6596/250/1/012055.

Lewis, F.W., Harwood, L.M., Hudson, M.J., Drew, M.G.B., Sypula, M., Modolo, G., Whittaker, D., Sharrad, C.A., Videva, V., Hubscher-Bruder, V., Arnaud-Neu, F., 2012. Complexation of lanthanides, actinides and transition metal cations with a 6-(1,2,4-triazin-3-yl)-2,2':6',2''-terpyridine ligand: implications for actinide (iii)/lanthanide(iii) partitioning. Dalton Trans. 41, 9209-9219.

Liosi, G.M., Gambarini, G., Artuso, E., Benedini, S., Macerata, E., Giacobbo, F., Gargano, M., Ludwig, N., Carrara, M., Pignoli, E., Mariani, M., 2015. Study of Fricke-gel dosimeter calibration for attaining precise measurements of the absorbed dose. In: Proceedings of the 4th International Conference on Advancements in Nuclear Instrumentation Measurement Methods and their Applications (ANIMMA), IEEE, DOI: http://dx.doi.org/10.1109/ANIMMA.2015.7465581

Marrale, M., Brai, M., Gagliardo, C., Gallo, S., Longo, A., Tranchina, L., Abbate, B., Collura, G., Gallias, K., Caputo, V., Casto, A.L., Midiri, M., D'Errico, F., 2014. Correlation between ferrous ammonium sulfate concentration, sensitivity and stability of Fricke gel dosimeters exposed to clinical X-ray beams. Nucl. Instrum. Methods Phys. Res. Sect. B: Beam Interact. Mater. At. 335, 54–60.

Olding, T., Holmes, O., Schreiner, L.J., 2010. Cone beam optical computed tomography for gel dosimetry I: scanner characterization. Phys. Med. Biol. 55 (10), 2819.

Schreiner, L.J., 2004. Review of Fricke gel dosimeters. J. Phys.: Conf. Ser. 3, 9–21. http://dx.doi.org/10.1088/1742-6596/3/1/003.

Vander Griend, D.A., Bediako, D.K., DeVries, M.J., DeJong, N.A., Heeringa, L.P., 2008. Detailed spectroscopic, thermodynamic, and kinetic characterization of Nickel(II) complexes with 2,2'-bipyridine and 1,10-phenanthroline attained via equilibrium-restricted factor analysis. Inorg. Chem. 47 (2), 656–662.